Annexin A6-Balanced Late Endosomal Cholesterol Controls Influenza A Replication and Propagation

Agnes Musiol,[a] Sandra Gran,[a] Christina Ehrhardt,[b] Stephan Ludwig,[b] Thomas Grewal,[c] Volker Gerke,[a] Ursula Rescher[a]

Institute of Medical Biochemistry, Centre for Molecular Biology of Inflammation and Interdisciplinary Clinical Research Centre, University of Münster, Münster, Germany[a]; Institute of Molecular Virology, Centre for Molecular Biology of Inflammation, University of Münster, Münster, Germany[b]; Faculty of Pharmacy A15, University of Sydney, Sydney, NSW, Australia[c]

ABSTRACT **Influenza is caused by influenza A virus (IAV), an enveloped, negative-stranded RNA virus that derives its envelope lipids from the host cell plasma membrane. Here, we examined the functional role of cellular cholesterol in the IAV infection cycle. We show that shifting of cellular cholesterol pools via the Ca^{2+}-regulated membrane-binding protein annexin A6 (AnxA6) affects the infectivity of progeny virus particles. Elevated levels of cellular AnxA6, which decrease plasma membrane and increase late endosomal cholesterol levels, impaired IAV replication and propagation, whereas RNA interference-mediated AnxA6 ablation increased viral progeny titers. Pharmacological accumulation of late endosomal cholesterol also diminished IAV virus propagation. Decreased IAV replication caused by upregulated AnxA6 expression could be restored either by exogenous replenishment of host cell cholesterol or by ectopic expression of the late endosomal cholesterol transporter Niemann-Pick C1 (NPC1). Virus released from AnxA6-overexpressing cells displayed significantly reduced cholesterol levels. Our results show that IAV replication depends on maintenance of the cellular cholesterol balance and identify AnxA6 as a critical factor in linking IAV to cellular cholesterol homeostasis.**

IMPORTANCE **Influenza A virus (IAV) is a major public health concern, and yet, major host-pathogen interactions regulating IAV replication still remain poorly understood. It is known that host cell cholesterol is a critical factor in the influenza virus life cycle. The viral envelope is derived from the host cell membrane during the process of budding and, hence, equips the virus with a special lipid-protein mixture which is high in cholesterol. However, the influence of host cell cholesterol homeostasis on IAV infection is largely unknown. We show that IAV infection success critically depends on host cell cholesterol distribution. Cholesterol sequestration in the endosomal compartment impairs progeny titer and infectivity and is associated with reduced cholesterol content in the viral envelope.**

Received 2 August 2013 **Accepted** 8 October 2013 **Published** 5 November 2013

Citation Musiol A, Gran S, Ehrhardt C, Ludwig S, Grewal T, Gerke V, Rescher U. 2013. Annexin A6-balanced late endosomal cholesterol controls influenza A replication and propagation. mBio 4(6):e00608-13. doi:10.1128/mBio.00608-13.

Invited Editor Stephan Pleschka, Justus-Liebig-University Giessen **Editor** Vincent Racaniello, Columbia University College of Physicians & Surgeons

Address correspondence to Ursula Rescher, rescher@uni-muenster.de.

Influenza A virus (IAV) remains a major public health concern, not only by causing thousands of deaths because of annual epidemics and rare but often severe pandemics but also by leading to enormous economic loss every year (1). As agents directed against viral components select for resistant mutants, new antiviral therapeutic approaches might target the interaction of virus with host cell components. Despite the enormous progress in influenza-related research in the last decade, major host-pathogen interactions regulating IAV replication and propagation still remain poorly understood. The virus is characterized by a segmented, single-stranded RNA genome with negative orientation, and its genome encodes up to 12 viral structural and nonstructural proteins (2). The virus genome is enclosed by an envelope that is derived from the host cell membrane during the process of budding and, hence, equips the virus with a special lipid-protein mixture. As this process is heavily dependent on the presence of specialized and cholesterol-enriched lipid microdomains, or so-called "rafts," this leads to a high level of cholesterol, a major component of those raft domains, in the virus envelope (3–7).

Host cell cholesterol is a critical factor in IAV replication and propagation. It is known that viral assembly and budding, as well as infectivity, are strongly dependent on cellular cholesterol levels, indicating the great importance of this host factor for virus infection (7–11). However, the molecular mechanisms of these regulatory interactions are largely unknown. This is partly due to the limited knowledge about intracellular cholesterol transport between distinct membrane compartments in the host cell that regulates cholesterol homeostasis, as well as cholesterol-sensitive protein trafficking (12).

Recently, annexin A6 (AnxA6) has emerged as an important player in the maintenance of cellular cholesterol homeostasis (13–16). Annexin A6 is a member of the annexin protein family of structurally highly conserved, Ca^{2+}-regulated membrane-binding proteins that have been linked to the regulation of membrane recognition and trafficking (17–20). All annexins share a common structure composed of two domains: a conserved core that is responsible for Ca^{2+} and phospholipid binding and an N-terminal tail that is unique for each annexin. Due to their role in

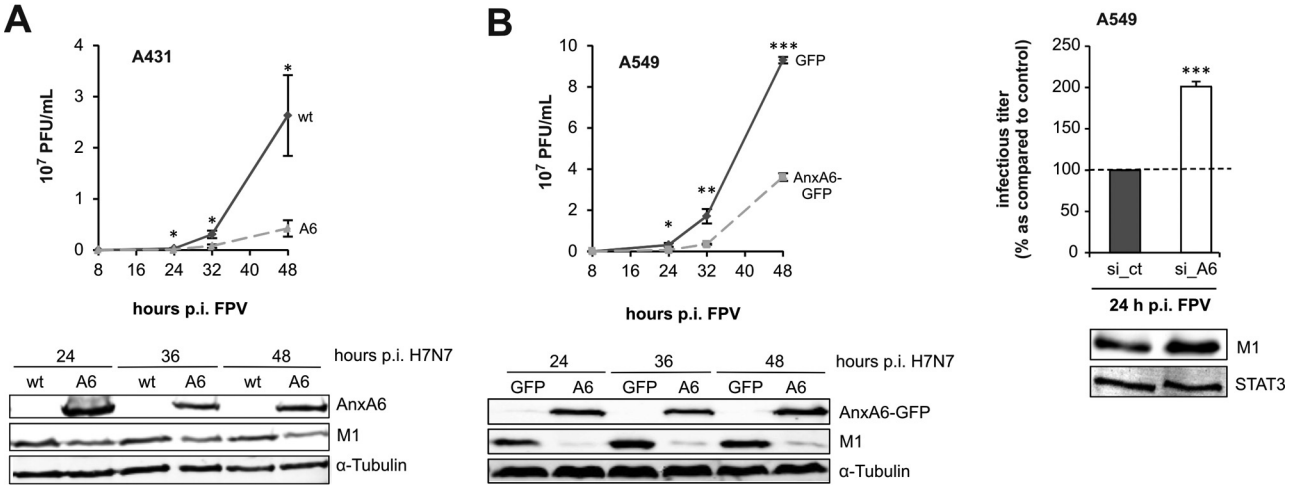

FIG 1 AnxA6 negatively modulates influenza A virus replication. A431 wild-type (wt) and A431 cells stably overexpressing AnxA6 (A6) (A), as well as A549 cells transiently overexpressing GFP or AnxA6-GFP (B, left), were infected with the avian IAV isolate A/FPV/Bratislava/79 (H7N7; FPV) at an MOI of 0.01. At the indicated time points postinfection (p.i.), progeny virus titers were determined by standard plaque assay. IAV M1 and AnxA6 protein levels in cell lysates were determined by Western blotting. Equal protein loading was verified by using α-tubulin. (B, right) A549 cells transfected with AnxA6 siRNA (si_A6) or nontargeting control siRNA (si_ct) were infected with FPV for 24 h at an MOI of 0.1, and viral progeny were determined by standard plaque assay. Levels of M1 and AnxA6 proteins were monitored by Western blotting, and blots were probed for STAT3 to verify equal protein loading. Mean values ± SEM of at least three independent experiments were calculated and assessed for statistically significant differences using a two-tailed *t* test. *, $P \leq 0.05$; **, $P \leq 0.01$; ***, $P \leq 0.001$.

membrane dynamics, annexins have already been shown to be involved in the life cycles of several pathogens, including diverse viruses. Regarding infections with IAV, proteomic analysis of influenza virions revealed the incorporation of annexins A1, A2, A4, A5, and A11 into IAV particles (21). For AnxA2, it was even reported that the protein has a supportive role for IAV replication (22, 23). Recently, AnxA6 was proposed to be negatively involved in IAV replication (24). Here, we elucidate the molecular mechanism through which annexin A6 exerts a strong antiviral effect. We show that AnxA6 affects the infectivity of progeny virus particles through shifting intracellular cholesterol pools. This effect was independent of the plasma membrane-associated pool of AnxA6 and could be reversed either through exogenous replenishment of host cell cholesterol or by overexpression of the late endosomal cholesterol transporter NPC1. These studies support a role for AnxA6 in IAV replication and propagation and indicate that cellular cholesterol homeostasis is critically linked to the infectivity of the virus.

RESULTS

Annexin A6 negatively modulates influenza virus replication. To examine the function of AnxA6 in IAV replication, we employed the human epithelial carcinoma cell line A431 (hereinafter called A431wt, for A431 wild type), which naturally lacks endogenous AnxA6, and the A431-A6 cell line, which has stable expression of AnxA6 (25, 26). Western blot analysis of cell lysates confirmed that the expression of AnxA6 was only detectable in A431-A6 cells (Fig. 1A, bottom). A431wt and A431-A6 cells were infected with the avian IAV isolate A/FPV/Bratislava/79 (H7N7; FPV) at a multiplicity of infection (MOI) of 0.01, and progeny virus titers were monitored over a time period of 48 h (Fig. 1A). The infectious titers of viruses produced by these cells and released into the cell culture supernatants were measured by a standard plaque assay technique. Both cell lines were permissive for IAV replication; however, in A431-A6 cells, the virus titers were impaired at every time point analyzed. This correlated with a reduced expression of virion-associated matrix protein 1 (M1), as assessed by Western blotting (Fig. 1A, bottom).

To confirm this result in a cell model relevant for infections of the upper respiratory tract and to exclude an aberrant phenotype as a consequence of clonal selection during A431-A6 cell line generation, we repeated this experiment using human A549 lung epithelial cells transiently transfected with green fluorescent protein (GFP)-tagged AnxA6 (A6-GFP) or GFP alone as a control. GFP and A6-GFP expression were verified by fluorescence microscopy (data not shown) and Western blotting (see Fig. S1 in the supplemental material). At 24 h after transfection, cells were infected as described above. Again, virus titers were significantly reduced in AnxA6-overexpressing cells (Fig. 1B). Furthermore, impaired viral progeny titers again correlated with reduced viral M1 protein expression. This observation strengthened the finding that elevated AnxA6 expression negatively influences IAV replication.

To further verify an involvement of AnxA6 in IAV replication, we performed small interfering RNA (siRNA)-mediated knockdown of AnxA6 in A549 cells using a pool of AnxA6-specific siRNA duplexes and nontargeting siRNA as a control. At 48 h after transfection, cells were infected with FPV at an MOI of 0.1, and virus replication was allowed to proceed for 24 h. Efficient and reproducible AnxA6 knockdown was confirmed by Western blot analysis (see Fig. S1 in the supplemental material). In line with a role of AnxA6 as a negative regulator, downregulation of AnxA6 resulted in significantly enhanced progeny virus titers in cell culture supernatants compared to the titers in control siRNA-treated cells (Fig. 1B, top right). This correlated with higher M1 virus protein expression.

Additional experiments revealed that AnxA6 also inhibited the replication of other influenza strains, such as the H1N1 IAV strain A/Puerto Rico/8/34 (PR8) and a mouse-adapted strain (H1N1v; HH/04-3rd) of the 2009 pandemic swine-origin influenza A virus

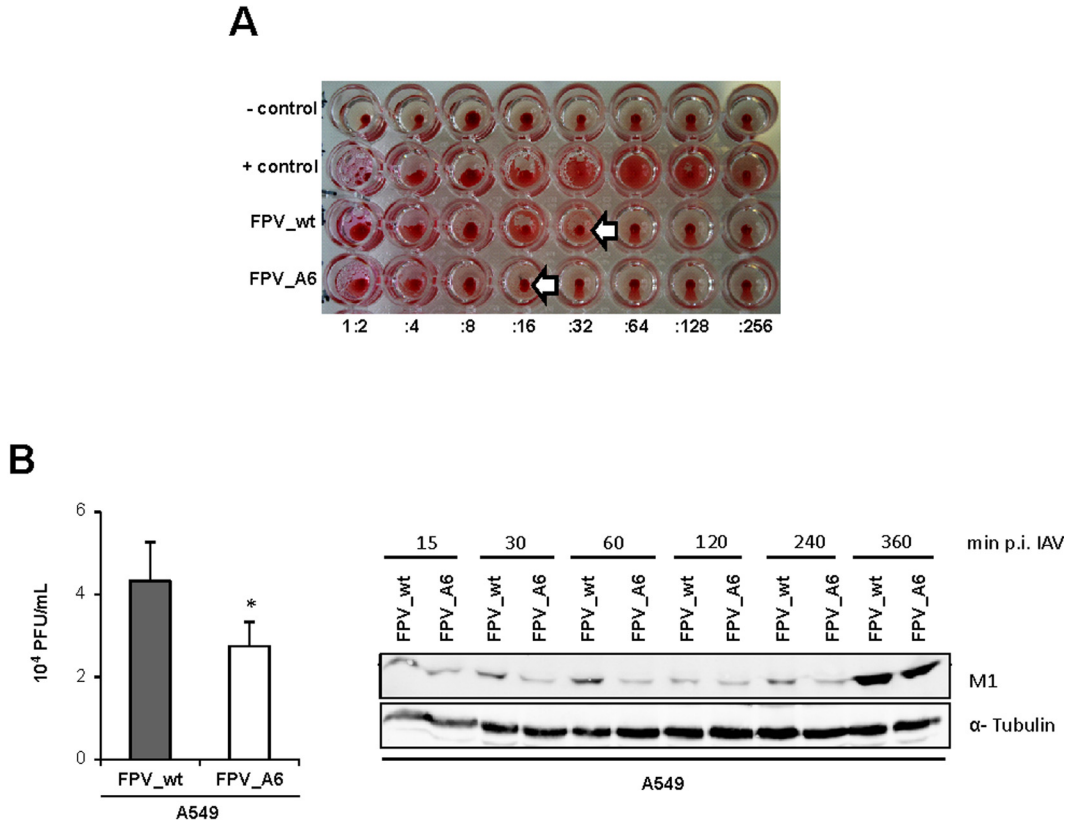

FIG 2 AnxA6 upregulation decreases the amount and infectivity of viral particles. (A) A431wt and A431-A6 cells were infected with FPV (MOI of 0.1 for 24 h), and supernatants obtained from either A431wt (FPV_wt) or A431-A6 (FPV_A6) cells were analyzed by hemagglutination assay. + control, positive control; − control, negative control. Arrows indicate the greatest serum dilution giving a visible agglutination. (B) A431wt and A431-A6 cells were infected with FPV (MOI of 0.1 for 48 h), and progeny virus titers were determined by standard plaque assay. A549 cells were then infected for 8 h with the virus replicated in A431wt (FPV_wt) or A431-A6 cells (FPV_A6). For determination of infectious viral titers, an MOI of 0.1 was used. To monitor virus entry, A549 cells were infected with an MOI of 5 for 15 to 360 min, as indicated. IAV M1 protein levels in cell lysates were monitored by Western blotting. Equal protein loading was verified using α-tubulin. Mean values ± SEM of at least three independent experiments were calculated and assessed for statistically significant differences using a two-tailed *t* test. *, $P \leq 0.05$.

subtype H1N1 variant (H1N1v) strain A/Hamburg/04/2009 (see Fig. S2 in the supplemental material).

Annexin A6 overexpression inhibits IAV particle production and decreases virus infectivity. So far, our results indicated an impact of cellular AnxA6 levels on IAV infection. To determine whether the decrease in progeny virus titers induced by AnxA6 overexpression was due to reduced infectivity or a decreased amount of infectious virus particles, we first performed hemagglutination (HA) assays to determine the levels of IAV particles present in the sample. For this purpose, we infected A431wt and A431-A6 cells with FPV at an MOI of 0.1, allowed the infection to proceed for 24 h, and used the resulting supernatants for the HA assay. As shown by the results in Fig. 2A, supernatants from infected A431wt cells (FPV_wt) caused hemagglutination of red blood cells up to the 1:32 dilution, whereas viral particles produced by A431-A6 cells (FPV_A6) needed the 1:16 dilution. Therefore, the amount of viral particles produced by A431-A6 cells was decreased by approximately 50% compared to the amount produced by controls. This strongly indicated that high AnxA6 levels inhibit the production of viral particles *per se*. However, an additional effect on infectivity could not be excluded, as the decrease in infectious titers in AnxA6-overexpressing cells appeared to be greater than the 50% decrease in the total production of IAV particles. To address the infectivity of IAV particles, we therefore reinfected A549 cells with virus obtained from infected A431wt (FPV_wt) or A431-A6 (FPV_A6) cells. To obtain one cycle of IAV replication, we allowed the infection to proceed for 8 h. Although A549 cells were infected with the same MOI of the respective virus (MOI of 0.1), the virus titers were still decreased in cells infected with virus that originated from A431-A6 cells (Fig. 2B, left). Next, we investigated the entry process of the respective virus into the host cell. Therefore, virion-associated matrix protein was detected by Western blot analysis, as described previously (27). We infected A549 cells with FPV_wt or FPV_A6 at an MOI of 5 and followed IAV internalization by detection of viral M1 protein (Fig. 2B, right). A549 cells infected with FPV_A6 showed a strong decrease in the amount of M1 protein compared to the amount in cells infected with FPV_wt, indicating that the virus produced in A431-A6 cells displayed reduced capability in the entry process and, hence, exhibited decreased infectivity of viral particles.

In conclusion, high levels of AnxA6 not only decreased the amount of viral particles produced by the host cell but, in addition, decreased the infectivity of those particles.

Plasma membrane-associated functions of AnxA6 are not responsible for its antiviral activity. Next, we aimed to investigate

the underlying mechanism by which high AnxA6 levels decreased the infectivity of IAV particles. Upon cell activation, AnxA6 binds to negatively charged phospholipids that are found predominantly in the plasma membrane but also in endosomal membranes. As AnxA6 is mainly localized at the plasma membrane, we first addressed a role for plasma membrane-associated AnxA6 for antiviral activity.

Recently, AnxA6 was found to target p120GAP and protein kinase Cα (PKCα) to the plasma membrane, thereby inactivating Ras and epidermal growth factor receptor (EGFR), respectively, and to downregulate the Raf/MEK/ERK (extracellular signal-regulated kinase) signaling cascade (28–31). As this signaling pathway is activated in a biphasic manner during IAV infections and is essential for virus production (32, 33), high levels of AnxA6 might lead to an inhibition of IAV replication by disturbing Raf/MEK/ERK signaling. To examine this possibility, we infected A431wt and A431-A6 cells (FPV at an MOI of 5) and monitored ERK1/2 activation by Western blotting. As shown by the results in Fig. 3A, the kinetics of ERK1/2 phosphorylation during infection proceeded in a similar manner in both cell lines.

Besides being a scaffold for EGFR and Ras signaling, AnxA6 exhibits further functions at the plasma membrane, as it associates with cholesterol-rich membrane microdomains termed lipid rafts and may function as an organizer of those domains to regulate transient membrane-actin interactions during endocytosis. Furthermore, AnxA6 has been shown to be involved in clathrin-mediated endocytosis, which is exploited by IAV to enter host cells (26, 34–37). To address whether AnxA6 might be involved in the entry process of IAV into the host cell, we monitored the kinetics of the appearance of the virion-associated matrix protein 1 (M1) in A549 cells expressing GFP or A6-GFP following infection (FPV at an MOI of 10). The M1 levels were comparable in AnxA6-overexpressing cells and controls, indicating that high levels of AnxA6 had no inhibitory effect on early stages of the viral life cycle (from entry to escape from late endosomes) (Fig. 3B).

The results described above suggested that plasma membrane-associated AnxA6 was not responsible for the antiviral activity. To confirm this, A549 cells were transfected with A6-GFP and membrane-anchored AnxA6-GFP (AnxA6-GFP-th, generated by the addition of the complete H-Ras membrane targeting signal) (16, 28, 38). GFP and plasma membrane-anchored GFP (GFP-th) served as controls. At 24 h after transfection, the cells were infected with FPV (MOI of 0.01 for 24 h). A6-GFP and A6-GFP-th expression levels were verified by fluorescence microscopy (data not shown) and Western blotting (see Fig. S1B in the supplemental material). As described above, the virus titers were decreased in cells overexpressing AnxA6 but not in cells expressing AnxA6-th compared to the titers in the respective control (Fig. 3C). Taken together, AnxA6 is not likely to engage in antiviral activity by interfering with virus entry and virus-induced mitogen-activated protein kinase (MAPK) signaling at the plasma membrane.

High levels of AnxA6 lead to cholesterol sequestration in A549 cells. Host cell cholesterol is a critical factor in IAV replication. Viral assembly and budding, as well as infectivity, are strongly dependent on cellular cholesterol distribution, indicating the great importance of this host factor for virus infection (3–5, 7). However, the molecular mechanisms underlying the link between cellular cholesterol and virus replication are largely unknown. Recently, AnxA6 was proposed to be involved in the regulation of cholesterol homeostasis: high levels of AnxA6 were shown to induce an NPC1-like phenotype, as characterized by an accumulation of cholesterol in late endosomes. Inhibition of cholesterol export from the late endocytic compartment in AnxA6-expressing cells was associated with reduced cholesterol levels in the Golgi apparatus and the plasma membrane (15, 16). These findings prompted us to investigate whether modulation of cholesterol homeostasis by AnxA6 could be responsible for the AnxA6-mediated inhibition of IAV replication.

To address this, we first compared the cholesterol distribution in AnxA6-overexpressing A549 cells and controls, as described previously (15, 16). A549 cells were transfected with A6-GFP or GFP, fixed, stained with filipin, and analyzed for their cellular cholesterol distribution by confocal microscopy. Treatment with U18666A, a hydrophobic polyamine known to promote the accumulation of cholesterol in late endosomes, served as a positive control. In control cells, cholesterol was detectable at the plasma membrane and in punctate structures throughout the cytoplasm. In contrast, the majority of A6-GFP-overexpressing cells showed a very different staining pattern. In particular, a much stronger accumulation of cholesterol in mostly perinuclear vesicles was observed (Fig. 4A). This accumulation resembled the scenario in U18666A-treated cells, indicating that the cholesterol accumulation in late endosomes observed previously in several AnxA6-overexpressing cell lines (15, 16) also holds true for AnxA6 overexpression in A549 cells.

Cholesterol accumulation in late endosomes is responsible for the inhibition of virus replication by AnxA6. We next investigated whether U18666A-induced late endosomal cholesterol accumulation could interfere with IAV propagation. Therefore, A549 cells were treated with and without U18666A overnight and infected with FPV at an MOI of 0.1, and virus replication was allowed to proceed for 24 h. The infectious titers of viruses produced in cell culture supernatants were measured by a standard plaque assay technique. Consistent with a model of inhibition of cholesterol egress from late endosomes blocking virus propagation, U18666A treatment and AnxA6 overexpression had strikingly similar inhibitory effects on infectious progeny virus titers (ca. 50%) (compare Fig. 4B and 2A). This correlated with the reduced expression of viral M1 protein in U18666A-treated A549 cells (Fig. 4B, bottom).

To further substantiate these findings, the progeny virus titers of A549 cells preincubated with and without U18666A overnight, infected with IAV at an MOI of 0.1 for 24 h, and ectopically expressing A6-GFP or GFP were compared. Consistent with the results described above, U18666A treatment significantly impaired the progeny virus titers of GFP-expressing A549 cells, and the M1 protein levels were downregulated in these cells (Fig. 4B). In AnxA6-GFP-overexpressing A549 cells, however, the addition of U18666A had only a minor inhibitory effect on infectious virus particles and M1 protein expression (Fig. 4C). Taken together, the inhibition of cholesterol export from late endosomes by U18666A treatment leads to significantly reduced progeny virus titers, strongly suggesting that the inhibitory effect of AnxA6 overexpression on IAV replication is due to an inhibition of cholesterol egress from late endosomes.

Restoration of cellular cholesterol balance in AnxA6-overexpressing cells restores influenza virus replication. AnxA6 is recruited to late endosomes in a cholesterol-dependent manner (13) and, possibly, through physical interaction with NPC1, which could block NPC1-dependent cholesterol export from the

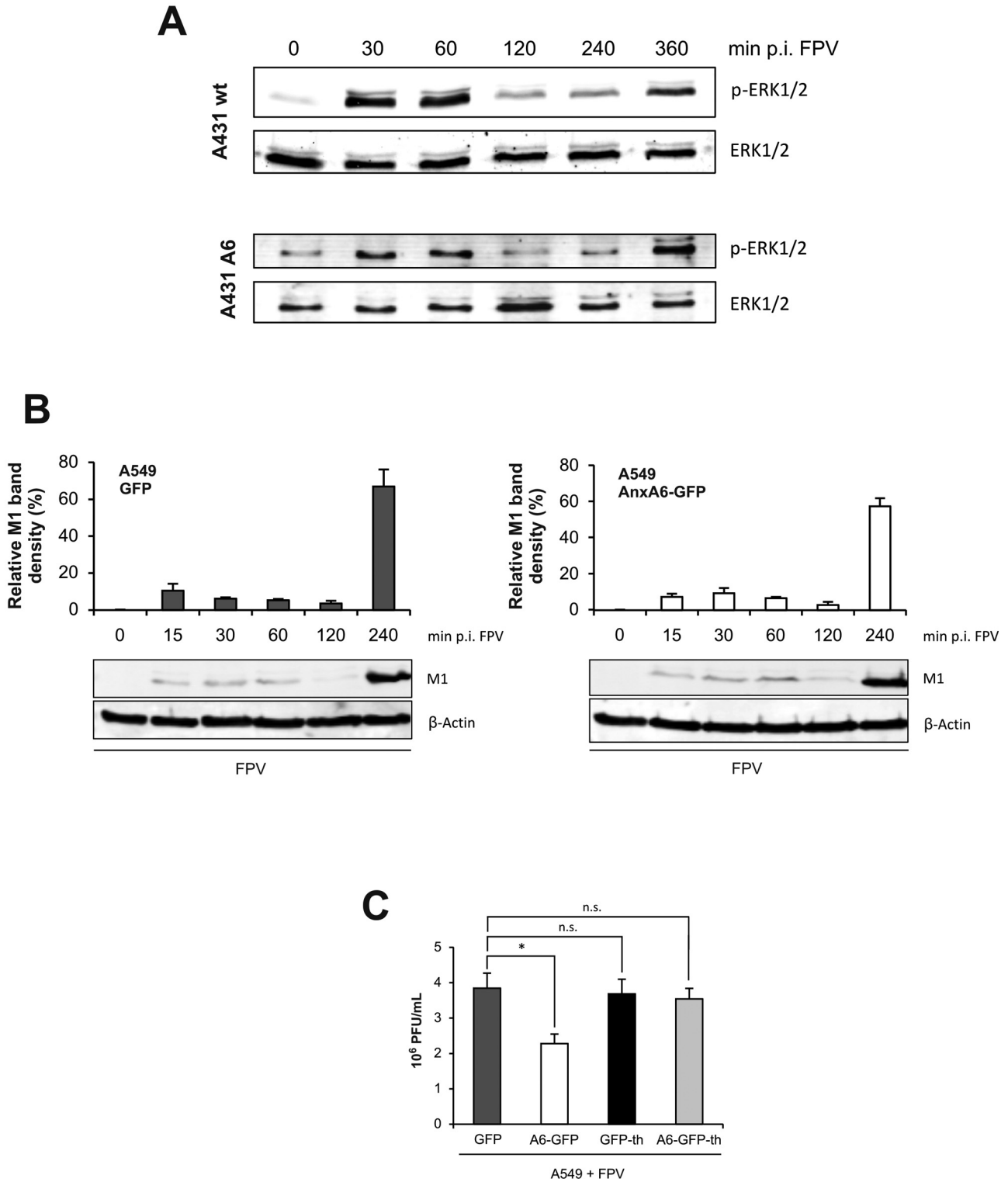

FIG 3 IAV entry and MAPK signaling are not altered in AnxA6-overexpressing cells. (A) A431wt and A431-A6 cells were starved in 1% FBS overnight and infected with FPV at an MOI of 5. Cells were lysed after 15 to 360 min, as indicated, and analyzed for total (ERK1/2) and phosphorylated ERK1/2 (p-ERK1/2) by Western blotting. (B) A549 cells transiently overexpressing GFP or AnxA6-GFP were infected with FPV at an MOI of 10 for 0 to 240 min, as indicated. After cell lysis, expression of IAV M1 protein was monitored by Western blotting and quantified. Mean values ± SEM were calculated from three independent experiments. β-Actin served as a loading control. (C) A549 cells transiently overexpressing GFP, AnxA6-GFP, or plasma membrane-anchored GFP (GFP-th) or AnxA6-GFP (AnxA6-GFP-th) were infected with FPV (MOI of 0.01 for 24 h), and progeny virus titers were determined by standard plaque assay. Mean values ± SEM of at least three independent experiments were calculated and assessed for statistically significant differences using one-way ANOVA followed by Dunnett's multiple comparison test. *, $P \leq 0.05$; n.s., not significant.

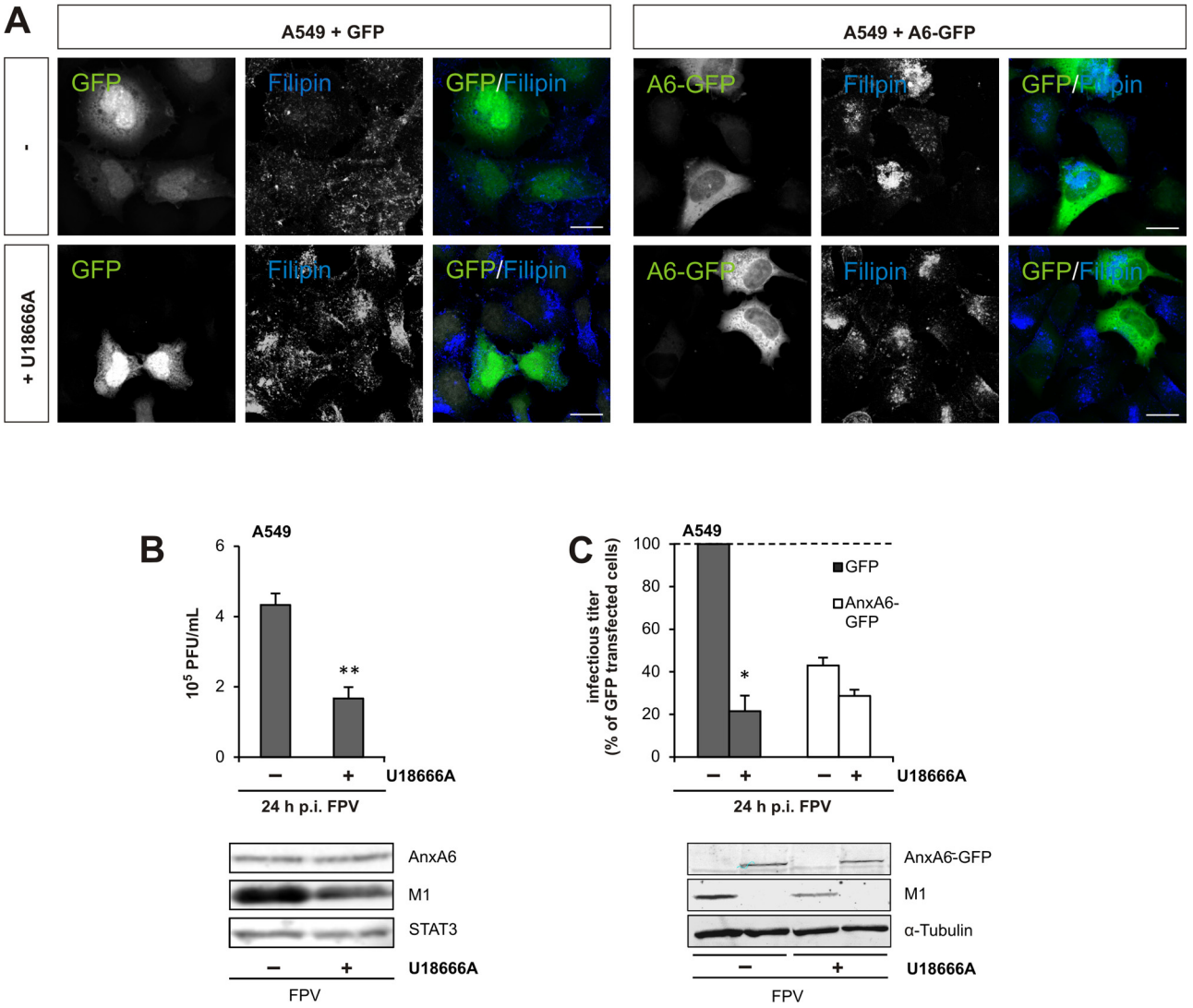

FIG 4 Pharmacological inhibition of late endosomal cholesterol egress inhibits influenza virus replication in A549 cells. (A) A549 cells transiently overexpressing GFP (green, left) or AnxA6-GFP (green, right) were treated with U18666A overnight. Cellular cholesterol was stained using filipin (blue). Bar, 20 μm. (B and C) A549 wild-type cells (B) or A549 cells transiently overexpressing GFP or AnxA6-GFP (C) were treated with U18666A overnight and then infected with FPV (MOI of 0.1 for 24 h). Progeny virus titers were determined by standard plaque assay. IAV M1 protein and AnxA6 expression levels were monitored by Western blotting. Equal protein loading was verified using STAT3 or α-tubulin, as indicated. Mean values ± SEM of at least three independent experiments were calculated and assessed for statistically significant differences using a two-tailed *t* test. *, $P \leq 0.05$; **, $P \leq 0.01$.

late endosomal/lysosomal compartment (15). Moreover, NPC1 overexpression restored the cellular cholesterol balance in AnxA6-overexpressing cells (15, 16). Given the findings described above, we reasoned that NPC1 overexpression could overcome the inhibitory effect of AnxA6 on viral replication. Therefore, A431-A6 cells were transiently transfected with an expression vector encoding yellow fluorescent protein (YFP)-tagged wild-type NPC1 (NPC1-YFP). NPC1-YFP expression was verified in duplicate samples by fluorescence microscopy (data not shown). At 24 h after transfection, cells were infected with FPV at an MOI of 0.1, and the infectious titers were measured with a standard plaque assay technique 24 h postinfection (p.i.). In support of our hypothesis, the overexpression of wild-type NPC1 partially restored progeny virus titers in A431-A6 cells (Fig. 5A). To further underscore this finding, we analyzed viral replication upon overexpression of the loss-of-function NPC1 P692S mutant (having a change of proline to serine at position 692), which cannot bind cholesterol and inhibits cholesterol export from late endosomes (39–41). Indeed, while IAV replication can be rescued by overexpression of wild-type NPC1, the P692S mutant was not able to reestablish viral titers in A431-A6 cells (Fig. 5B). P962S also significantly impaired IAV replication in A431wt cells (not shown), further suggesting that cholesterol pools from late endosomes are required for efficient virus replication and propagation.

Inhibition of late endosomal cholesterol export reduces cholesterol levels in other cellular compartments, such as the plasma membrane. We speculated that the reduction of cholesterol levels at the plasma membrane triggered by AnxA6, U18666A, or the NPC1 mutant could be responsible for reducing viral propagation. To address this possibility, A549 cells were transiently trans-

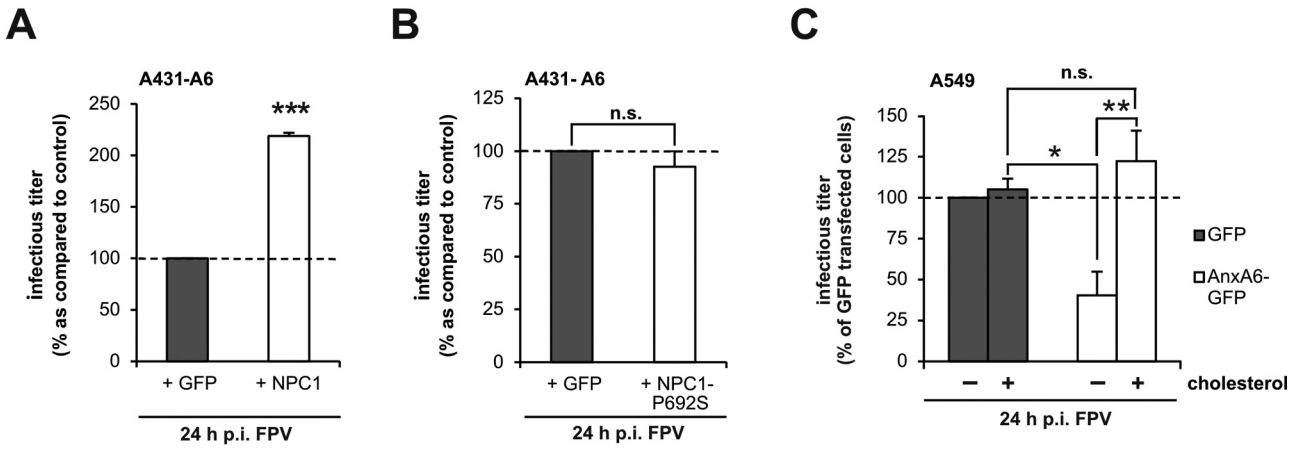

FIG 5 Restoration of late endosomal cholesterol export restores IAV titers. (A and B) A431-A6 cells transiently expressing NPC1-YFP (A) or NPC1 P692S-YFP (B) were infected with FPV (MOI of 0.1 for 24 h). Progeny virus titers were determined by standard plaque assay. (C) A549 cells transiently overexpressing GFP or AnxA6-GFP were infected with FPV (MOI of 0.1 for 24 h). Exogenous cholesterol was added to the medium at 2 h p.i. Progeny virus titers were determined by standard plaque assay and expressed as percentages of virus titers released from GFP-expressing control cells. Statistically significant differences of the mean values ± SEM calculated from at least three independent experiments were assessed by two-tailed *t* test (A, B) or by one-way ANOVA followed by Tukey's multiple comparison test (C). *, $P \leq 0.05$; **, $P \leq 0.01$; ***, $P \leq 0.001$; n.s., not significant.

fected with A6-GFP or GFP, followed by the addition of exogenous cholesterol to replenish plasma membrane cholesterol. Next, cholesterol-treated and nontreated A549 cells were infected with FPV at an MOI of 0.1, and the infectious titers were measured with the standard plaque assay technique. Indeed, cholesterol replenishment completely restored the progeny virus titers in A6-GFP-overexpressing A549 cells (Fig. 5C), further supporting a role for AnxA6 to modulate cholesterol-dependent steps during viral replication. In conclusion, restoration of the cellular cholesterol balance via cholesterol replenishment using exogenous cholesterol or the ectopic expression of wild-type NPC1 in AnxA6-overexpressing cells improves the ability of IAV to replicate and propagate.

IAV cholesterol content is decreased in viral progeny released from cholesterol-imbalanced host cells. The data described above strongly indicated a role for cholesterol in the antiviral effect of elevated AnxA6 contents. Budding from cholesterol-rich sites at the plasma membrane provides the virus with a cholesterol-rich envelope (6, 42). Hence, we assessed whether altered cholesterol distribution in A431-A6 cells had an impact on the cholesterol levels in the viral envelope. We therefore compared the cholesterol contents of purified IAV released from A431 and A431-A6 cells at 24 h p.i. The purity of IAV preparations was controlled by verifying the absence of the viral nonstructural protein NS1 in Western blots (Fig. 6A). As shown by the results in Fig. 6B, comparable amounts of cholesterol were detected in the lysates of both cell lines before and after infection. However, virus particles released from A431-A6 cells displayed a 50% reduction in cholesterol content, indicating that cholesterol sequestration in late endosomes and the concomitant decrease in cholesterol at the cell periphery leads to less cholesterol being available for viral budding and envelope formation.

DISCUSSION

The dynamics of membrane events and signaling are intimately linked to the interactions of proteins with lipids and lipid domains (43). Thus, many pathogens, including viruses, employ host cell lipid-enriched microdomains at different points of their infection process to efficiently infect the target cell (44). Like other enveloped viruses, IAV depends on the host membrane and its dynam-

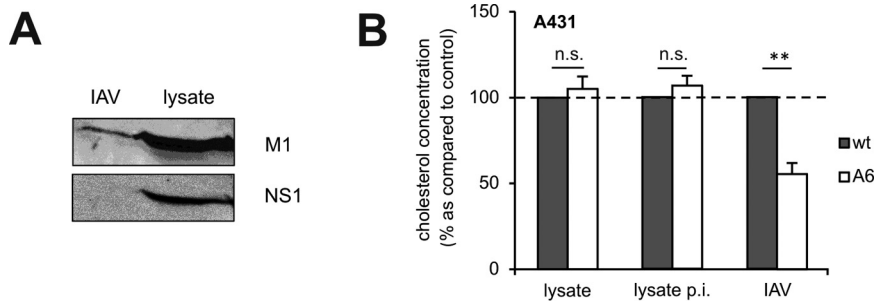

FIG 6 High levels of AnxA6 significantly decrease the cholesterol content in the viral envelope. A431wt and A431-A6 cells were infected with FPV (MOI of 0.1) or mock treated with infection medium. At 24 h p.i., supernatants were concentrated, purified, and assayed, together with the respective cell lysates, for their cholesterol content. (A) Purity of IAV preparations was verified by the exclusion of the viral nonstructural protein NS1 from virus samples in Western blots. (B) Cholesterol content in cell lysates and viral particles (IAV) released from A431wt (wt) and A431-A6 cells (A6) before and after (p.i.) infection. Statistically significant differences of the mean values ± SEM calculated from at least three independent experiments were assessed by Student's *t* test. **, $P \leq 0.01$; n.s., not significant.

ics at several stages of the viral life cycle. Annexins constitute a family of Ca^{2+}-dependent host cell membrane proteins that have different lipid specificities and, thus, associate with different target membranes in the cell (17–19, 45). Annexins have already been shown to act in viral infections (46), and IAV carries several annexins in its particle, most likely as a consequence of budding at raftlike domains enriched with annexins (22, 23).

Recently, AnxA6 has been proposed to negatively regulate IAV infection through interaction with the IAV matrix protein M2 (24). Here, we show that AnxA6 levels in the host cell negatively correlate with IAV replication and reveal that aberrant cholesterol accumulation in late endosomes, reminiscent of an NPC1 mutant-like phenotype, in AnxA6-expressing cells causes antiviral activity. Consistently, when cells were treated with the hydrophobic polyamine U18666A, a drug commonly used to mimic the abnormal accumulation of unesterified cholesterol seen in late endosomes of NPC1 mutant cells (47), a strong reduction in virus titers was observed. These findings suggest that AnxA6 interferes with NPC1-dependent cholesterol trafficking. In accordance with this, increased expression of wild-type NPC1, known to correct the NPC1 mutant-like phenotype in AnxA6-expressing cells (15, 16), significantly improved the virus titers in AnxA6-overexpressing cells. Cellular cholesterol is synthesized *de novo* in the endoplasmic reticulum (ER) and transported to the plasma membrane independently of NPC1 (47). Subsequently, it reinternalizes to the ER or other cellular compartments and/or recycles back to the plasma membrane. Dysfunctional NPC1 disturbs the intracellular distribution of cholesterol, leading to its accumulation in late endosomes and a secondary reduction of cholesterol levels in other cellular sites, such as the Golgi apparatus and the plasma membrane. This is also observed in AnxA6-overexpressing cells (15). The fact that AnxA6 coimmunoprecipitates with NPC1 suggests that a direct interaction of these proteins in the late endocytic compartment interferes with the ability of NPC1 to bind and transfer cholesterol across the late endosomal/lysosomal membrane. Our finding that exogenous cholesterol partially reversed the inhibitory effect of AnxA6 on IAV propagation indicates that cellular cholesterol trafficking from the late endosome to other sites, most likely the plasma membrane, is required for efficient IAV replication. These results also argue against a major impact of other lipids, such as sphingosine, that have been found to accumulate abnormally together with cholesterol in the endo-/lysosomes of NPC mutant cells (48–50).

Over the past decade, cholesterol has been shown to be a crucial host factor for IAV. It is assumed that this essential host membrane component plays a decisive role during virus replication (10, 11, 42). Within the host cell membrane, cholesterol functions in intracellular transport and cell signaling, acting through lipid rafts. These cholesterol-enriched membrane microdomains have been implicated in several steps of the viral life cycle, including the assembly and budding of progeny virus particles at the plasma membrane (42). However, experimental evidence for the importance of rafts in IAV replication is mainly derived from detergent extraction experiments, which drastically change the distribution and potential clustering of certain lipids and proteins. More-conclusive evidence that plasma membrane rafts are involved in HA clustering is drawn from recent improvements in fluorescence microscopy techniques that allowed the analysis of protein-raft association in a more-physiological cellular membrane environment (51).

In contrast to other enveloped viruses that depend on host cell components to ensure budding and the release of viral progeny, IAV uses the virus-encoded M2 protein to mediate scission of buds (52). Although IAV is thought to bud from cholesterol-rich membrane domains, M2 was shown to partition into rafts only when clustered with HA (51). Physical association of AnxA6 with M2 has been reported previously (24) and was proposed to impair IAV replication in AnxA6-overexpressing cells. However, our data strongly suggest that AnxA6-mediated changes in cholesterol homeostasis also have to be considered, as the restoration of cellular cholesterol distribution, through NPC1 overexpression or the addition of exogenous cholesterol, reversed impaired IAV replication in AnxA6-overexpressing cells. This may point at AnxA6 exerting multiple functions in different cellular locations that either directly (M2) or indirectly (cholesterol) inhibit viral replication and propagation. It is tempting to speculate that the drop in virus titers observed in the previous study (24) was also accompanied by major alterations in cholesterol distribution caused by AnxA6 up-/downregulation, as described here. As AnxA6 displays enhanced binding to membranes with elevated cholesterol levels (13, 26, 53, 54), the interaction of AnxA6 with M2 could serve to facilitate M2 targeting to the IAV bud zone to ensure the assembly of virus components.

Host membrane-derived IAV envelope is enriched in lipids generally found in raft microdomains, including cholesterol. In fact, 44% of the total virus lipid is cholesterol, which represents approximately 12% of the total mass of the virion (6, 42). Budding of virus particles through rafts equips the particle with an appropriate lipid mixture that protects particles from environmental damage and, in the case of cholesterol, might promote membrane fusion upon virus entry. Hence, virus treated with cholesterol-depleting agents shows reduced infectivity (10). Our results now demonstrate that the AnxA6-mediated endosomal cholesterol sequestration that leads to reduced cholesterol contents in the plasma membrane (15) is associated with strongly reduced IAV cholesterol contents and impaired infectivity.

A precise understanding of the molecular mechanisms that underlie virus-host cell interactions is a prerequisite for targeting host cell components and could open up efficient therapeutic strategies. Antiviral drugs could circumvent the time-consuming vaccine development and the viral resistance due to rapid antigenic mutation. Host cell factor targeting has recently emerged as a promising approach (reviewed in reference 55), and recent findings strongly suggest that modulating the host immune response reduces mortality rates (56, 57). Thus, combination therapy of two or more antiviral drugs with different modes of action (i.e., targeting the virus and the host cell) to prevent and control acute infection could become the therapeutic approach of choice not only for IAV but also for other microbial infections. Statin treatment of hospitalized influenza patients is associated with reduced mortality (58), although it is difficult to distinguish between the immunosuppressive and the cholesterol-lowering effects. Targeting host cell components could provide an elegant approach to dissect and functionally address the influence of cellular cholesterol levels on IAV infection. Collectively, our data provide evidence that host cell factors, such as AnxA6, involved in maintaining proper cholesterol homeostasis have a major impact on IAV replication. We conclude that AnxA6 indirectly regulates IAV replication by reducing the availability of cholesterol at the plasma membrane, thereby equipping the budding virus with an envelope

that is strongly reduced in cholesterol. Thus, targeting the cellular cholesterol balance might ameliorate IAV infection. It remains to be determined whether additional defects in the delivery and/or assembly of viral components and cell surface molecules engaged in influenza release contribute to the reduced IAV replication.

MATERIALS AND METHODS

Cells, viruses, and infection conditions. The human alveolar epithelial cell line A549, the human epithelial carcinoma cell line A431 (A431wt), and A431-derived A431-A6 cells were cultivated in Dulbecco's modified Eagle's medium (DMEM). The generation of stable AnxA6-expressing A431 (A431-A6) cells has been described previously (31). Madin-Darby canine kidney (MDCK) cells were cultured in minimal essential medium (MEM). Cell culture media were supplemented with 10% heat-inactivated fetal bovine serum, 100 U/ml penicillin, and 0.1 mg/ml streptomycin. All cell lines were cultured at 37°C in a humidified 5% CO_2 atmosphere.

The avian influenza virus A/FPV/Bratislava/79 (H7N7; FPV) and the human prototype strain A/Puerto Rico/8/34 (H1N1) (PR8) were originally obtained from the virus strain collection of the Institute of Virology, Giessen, Germany. The mouse-adapted S-OIV A/Hamburg/04/2009 (H1N1v) strain (H1N1v; HH/04-3rd), adapted to efficient propagation in mice by sequential lung-to-lung passages, was generated in house (59). All viruses were propagated in MDCKII cells. For infection, cells were washed with phosphate-buffered saline (PBS) and incubated with the respective virus at the indicated multiplicities of infection (MOI) diluted in PBS-BA (PBS containing 0.2% bovine serum albumin [BSA; MP Biomedicals], 1 mM $MgCl_2$, 0.9 mM $CaCl_2$, 100 U/ml penicillin, and 0.1 mg/ml streptomycin) at 37°C. After 30 min, the inoculum was aspirated, and cells were washed with PBS and incubated with DMEM-BA (DMEM containing 0.2% BSA, 1 mM $MgCl_2$, 0.9 mM $CaCl_2$, 100 U/ml penicillin, and 0.1 mg/ml streptomycin) for the times indicated.

Plaque titration. To quantify virus production, supernatants of infected cells were collected at the indicated times postinfection (p.i.) in duplicate experiments to assess the number of infectious particles by a standard plaque assay technique. For this purpose, MDCK cells grown to a monolayer in six-well dishes were washed with PBS and infected with serial dilutions of the respective supernatants in PBS-BA for 30 min at 37°C. The inoculum was replaced with 2 ml MEM-BA (MEM containing 0.2% BSA, 1 mM $MgCl_2$, 0.9 mM $CaCl_2$, 100 U/ml penicillin, and 0.1 mg/ml streptomycin) containing 0.6% agar (Oxoid, Hampshire, United Kingdom), 0.3% DEAE-dextran (Amersham Pharmacia Biotech, Freiburg, Germany), and 1.5% $NaHCO_3$ (Gibco Invitrogen, Karlsruhe, Germany) and incubated at 37°C. After 2 days, virus plaques were visualized by staining with neutral red. Virus titers were depicted as PFU/ml.

HA assay. Hemagglutination (HA) assays were performed in V-bottomed microtiter plates. Briefly, serial 2-fold dilutions of virus supernatants in PBS were prepared in microtiter plates in a volume of 50 μl. Additionally, PBS was used as a negative control and purified virus as a positive control. Amounts of 50 μl of chicken erythrocytes were added to the wells and were analyzed following 1 h of incubation at 4°C. Hemagglutination was observed with the unaided eye and monitored by photography.

Virus purification. For purification of IAV particles, harvested cell culture supernatants were first clarified by centrifugation (10 min at 700 $\times$ *g*) and then concentrated by using Centricon plus 70 filter devices (Millipore). For this purpose, the filter devices were coated with 1 mg/ml BSA overnight prior to virus concentration according to the manufacturer's instructions.

Cholesterol quantification. The cholesterol contents in cell lysates and IAV preparations were measured by using the Amplex red cholesterol assay kit (Invitrogen) according to the manufacturer's protocol. The results were normalized to total cellular protein.

Transient transfections, plasmids, and siRNAs. A549 and A431 cell lines were transfected with plasmid or siRNA using Lipofectamine 2000 (Invitrogen) according to the manufacturer's protocol. Human AnxA6 was expressed from the plasmid pEGFP-N1 (38), and murine NPC1 was expressed from the plasmid pEYFP-N2 (39). pEGFP-N3 served as a control. AnxA6 fused to the H-Ras membrane anchor was expressed from the pC1-based GFP-th plasmid. The cloning is described in detail in reference 38. Transfected cells were incubated for 24 h before the start of experiments. Transfection efficiency was controlled by fluorescence microscopy, as well as by detection of the respective proteins with Western blotting. For knockdown of AnxA6 protein expression, siRNA against human AnxA6 (siGENOME SMART pool, human ANXA6; Dharmacon) was used. Nontargeting siRNA (ON-Target plus siControl; Dharmacon) served as a negative control. Transfected cells were incubated for 48 h before the start of experiments, and transfection efficiency was controlled by using Western blots.

Cell lysis and Western blotting. After infection for the indicated times, cells were washed and harvested in 1.5 ml PBS and subsequently pelleted by centrifugation (15,000 $\times$ *g* for 1 min), resuspended in an appropriate amount of 8 M urea, and sonified. The protein concentration in the lysates was determined by the Bradford method. Cell lysates were used for protein expression analysis by SDS-PAGE and Western blotting. The primary antibodies used for detection of the respective proteins were mouse anti-influenza M1 monoclonal antibody (MAb) (AbD Serotec), mouse anti-annexin A6 MAb (BD Transduction Laboratories), mouse anti-α-tubulin MAb (Sigma-Aldrich), rabbit anti-GFP polyclonal antibody (PAb) (Invitrogen), rabbit anti-β-actin PAb (Sigma-Aldrich), rabbit anti-STAT3 MAb (Cell Signaling), mouse anti-MAPK p44/42 MAb (L34F12; Cell Signaling), and rabbit anti-phospho-MAPK p44/42 MAb (Thr202/Tyr204, D13.14.4E; Cell Signaling). Rabbit anti-AnxA6 PAb was prepared in our laboratory and has been described elsewhere (13, 26). IRDye secondary antibodies (LI-COR) labeled with near infrared (NIR) fluorescent dyes used for direct, nonenzymatic detection of primary antibodies were as follows: IRDye 680CW donkey anti-mouse IgG (H+L), IRDye 800CW donkey anti-mouse IgG (H+L), IRDye 680CW donkey anti-rabbit IgG (H+L), and IRDye 800CW donkey anti-rabbit IgG (H+L). The Odyssey infrared imaging system (LI-COR) was used for NIR fluorescence detection.

Quantification of Western blots. Western blots were quantified using the Odyssey infrared imaging system software version 3.0.25. The total band densities were measured against the local background. M1 signal intensities were normalized to β-actin. All data are expressed as the means of three independent transfection and infection experiments.

Filipin staining and microscopy. A549 cells destined for fluorescence microscopy were fixed with 4% paraformaldehyde (PFA)-PBS for 10 min at room temperature. For visualization of free cholesterol, fixed cells were blocked with 2% BSA for 30 min, incubated with filipin (filipin complex from *Streptomyces filipinensis*, diluted 1:50 in heat-inactivated fetal calf serum; Sigma-Aldrich), and washed with PBS. Confocal microscopy was carried out using an LSM 710 META microscope (Carl Zeiss, Jena, Germany) equipped with a Plan-Apochromat 63×/1.4 oil immersion objective.

Treatment with exogenous cholesterol or U18666A. For cholesterol replenishment experiments, water-soluble cholesterol (45 mg cholesterol complexed with 955 mg methyl-β-cyclodextrin [MβCD]; Sigma) was used. In brief, cholesterol was premixed for 60 min in DMEM-BA (30 μg/ml) and added to cells to a final concentration of 5 μg/ml 2 h after infection. For the accumulation of cholesterol in late endosomes, cells were treated for 16 h with 2 μg/ml U18666A (Biomol). If the cells were used for virus experiments, the infection of cells was followed by renewed treatment with 2 μg/ml U18666A. Filipin staining was used to control the late endosomal accumulation of free cholesterol upon U18666A treatment.

Statistical analysis. All experiments were performed at least three times, and mean values $\pm$ standard errors of the means (SEM) were calculated. Statistical significance was evaluated by two-tailed *t* test or by one-way analysis of variance (ANOVA) followed by either Tukey's or

Dunnett's multiple comparison test. A P value of <0.05 indicated a statistically significant difference.

SUPPLEMENTAL MATERIAL

Supplemental material for this article may be found at http://mbio.asm.org/lookup/suppl/doi:10.1128/mBio.00608-13/-/DCSupplemental.

Figure S1, TIF file, 0.2 MB.

Figure S2, TIF file, 0.3 MB.

ACKNOWLEDGMENTS

This work was supported by grants from the Interdisciplinary Clinical Research Center (IZKF; grant RE2/017/10) and the German Research Foundation (GRK 1409, RE2611/2-1, SFB 1009/A6, and SFB 629/A1) to U.R. and V.G. T.G. acknowledges support from the National Health and Medical Research Council of Australia (NHMRC; grant 510294) and the University of Sydney (grant 2010-02681).

REFERENCES

1. **Forrest HL, Webster RG.** 2010. Perspectives on influenza evolution and the role of research. Anim. Health Res. Rev. **11:**3–18.
2. **Cheung TK, Poon LL.** 2007. Biology of influenza A virus. Ann. N. Y. Acad. Sci. **1102:**1–25.
3. **Scheiffele P, Rietveld A, Wilk T, Simons K.** 1999. Influenza viruses select ordered lipid domains during budding from the plasma membrane. J. Biol. Chem. **274:**2038–2044.
4. **Simpson-Holley M, Ellis D, Fisher D, Elton D, McCauley J, Digard P.** 2002. A functional link between the actin cytoskeleton and lipid rafts during budding of filamentous influenza virions. Virology **301:**212–225.
5. **Zhang J, Pekosz A, Lamb RA.** 2000. Influenza virus assembly and lipid raft microdomains: a role for the cytoplasmic tails of the spike glycoproteins. J. Virol. **74:**4634–4644.
6. **Lenard J, Compans RW.** 1974. The membrane structure of lipid-containing viruses. Biochim. Biophys. Acta **344:**51–94.
7. **Nayak DP, Barman S.** 2002. Role of lipid rafts in virus assembly and budding. Adv. Virus Res. **58:**1–28.
8. **Nayak DP, Hui EK, Barman S.** 2004. Assembly and budding of influenza virus. Virus Res. **106:**147–165.
9. **Gerl MJ, Sampaio JL, Urban S, Kalvodova L, Verbavatz JM, Binnington B, Lindemann D, Lingwood CA, Shevchenko A, Schroeder C, Simons K.** 2012. Quantitative analysis of the lipidomes of the influenza virus envelope and MDCK cell apical membrane. J. Cell Biol. **196:**213–221.
10. **Sun X, Whittaker GR.** 2003. Role for influenza virus envelope cholesterol in virus entry and infection. J. Virol. **77:**12543–12551.
11. **Veit M, Thaa B.** 2011. Association of influenza virus proteins with membrane rafts. Adv. Virol. 2011:370606. doi:10.1155/2011/370606.
12. **Ikonen E.** 2008. Cellular cholesterol trafficking and compartmentalization. Nat. Rev. Mol. Cell Biol. **9:**125–138.
13. **de Diego I, Schwartz F, Siegfried H, Dauterstedt P, Heeren J, Beisiegel U, Enrich C, Grewal T.** 2002. Cholesterol modulates the membrane binding and intracellular distribution of annexin 6. J. Biol. Chem. **277:**32187–32194.
14. **Cubells L, Vilà de Muga S, Tebar F, Bonventre JV, Balsinde J, Pol A, Grewal T, Enrich C.** 2008. Annexin A6-induced inhibition of cytoplasmic phospholipase A2 is linked to caveolin-1 export from the Golgi. J. Biol. Chem. **283:**10174–10183.
15. **Cubells L, Vilà de Muga S, Tebar F, Wood P, Evans R, Ingelmo-Torres M, Calvo M, Gaus K, Pol A, Grewal T, Enrich C.** 2007. Annexin A6-induced alterations in cholesterol transport and caveolin export from the Golgi complex. Traffic **8:**1568–1589.
16. **Reverter M, Rentero C, de Muga SV, Alvarez-Guaita A, Mulay V, Cairns R, Wood P, Monastyrskaya K, Pol A, Tebar F, Blasi J, Grewal T, Enrich C.** 2011. Cholesterol transport from late endosomes to the Golgi regulates t-SNARE trafficking, assembly, and function. Mol. Biol. Cell **22:**4108–4123.
17. **Gerke V, Moss SE.** 2002. Annexins: from structure to function. Physiol. Rev. **82:**331–371.
18. **Gerke V, Creutz CE, Moss SE.** 2005. Annexins: linking Ca2+ signalling to membrane dynamics. Nat. Rev. Mol. Cell Biol. **6:**449–461.
19. **Rescher U, Gerke V.** 2004. Annexins—unique membrane binding proteins with diverse functions. J. Cell Sci. **117:**2631–2639.
20. **Enrich C, Rentero C, de Muga SV, Reverter M, Mulay V, Wood P, Koese M, Grewal T.** 2011. Annexin A6-linking ca(2+) signaling with cholesterol transport. Biochim. Biophys. Acta **1813:**935–947.
21. **Shaw ML, Stone KL, Colangelo CM, Gulcicek EE, Palese P.** 2008. Cellular proteins in influenza virus particles. PLoS Pathog. **4:**e1000085. doi:10.1371/journal.ppat.1000085.
22. **LeBouder F, Morello E, Rimmelzwaan GF, Bosse F, Péchoux C, Delmas B, Riteau B.** 2008. Annexin II incorporated into influenza virus particles supports virus replication by converting plasminogen into plasmin. J. Virol. **82:**6820–6828.
23. **LeBouder F, Lina B, Rimmelzwaan GF, Riteau B.** 2010. Plasminogen promotes influenza A virus replication through an annexin 2-dependent pathway in the absence of neuraminidase. J. Gen. Virol. **91:**2753–2761.
24. **Ma H, Kien F, Manière M, Zhang Y, Lagarde N, Tse KS, Poon LL, Nal B.** 2012. Human annexin A6 interacts with influenza A virus protein M2 and negatively modulates infection. J. Virol. **86:**1789–1801.
25. **King IC, Sartorelli AC.** 1986. The relationship between epidermal growth factor receptors and the terminal differentiation of A431 carcinoma cells. Biochem. Biophys. Res. Commun. **140:**837–843.
26. **Grewal T, Heeren J, Mewawala D, Schnitgerhans T, Wendt D, Salomon G, Enrich C, Beisiegel U, Jäckle S.** 2000. Annexin VI stimulates endocytosis and is involved in the trafficking of low density lipoprotein to the prelysosomal compartment. J. Biol. Chem. **275:**33806–33813.
27. **Eierhoff T, Ludwig S, Ehrhardt C.** 2009. The influenza A virus matrix protein as a marker to monitor initial virus internalisation. Biol. Chem. **390:**509–515.
28. **Koese M, Rentero C, Kota BP, Hoque M, Cairns R, Wood P, Vilà de Muga S, Reverter M, Alvarez-Guaita A, Monastyrskaya K, Hughes WE, Swarbrick A, Tebar F, Daly RJ, Enrich G, Grewal T.** 2012. Annexin A6 is a scaffold for PKCalpha to promote EGFR inactivation. Oncogene **32:**2858–2872.
29. **Grewal T, Koese M, Rentero C, Enrich C.** 2010. Annexin A6—regulator of the EGFR/ras signalling pathway and cholesterol homeostasis. Int. J. Biochem. Cell Biol. **42:**580–584.
30. **Grewal T, Enrich C.** 2006. Molecular mechanisms involved in ras inactivation: the annexin A6-p120GAP complex. Bioessays **28:**1211–1220.
31. **Grewal T, Evans R, Rentero C, Tebar F, Cubells L, de Diego I, Kirchhoff MF, Hughes WE, Heeren J, Rye KA, Rinninger F, Daly RJ, Pol A, Enrich C.** 2005. Annexin A6 stimulates the membrane recruitment of p120GAP to modulate ras and raf-1 activity. Oncogene **24:**5809–5820.
32. **Eierhoff T, Hrincius ER, Rescher U, Ludwig S, Ehrhardt C.** 2010. The epidermal growth factor receptor (EGFR) promotes uptake of influenza A viruses (IAV) into host cells. PLoS Pathog. **6:**e1001099. doi:10.1371/journal.ppat.1001099.
33. **Pleschka S, Wolff T, Ehrhardt C, Hobom G, Planz O, Rapp UR, Ludwig S.** 2001. Influenza virus propagation is impaired by inhibition of the raf/MEK/ERK signalling cascade. Nat. Cell Biol. **3:**301–305.
34. **Kamal A, Ying Y, Anderson RG.** 1998. Annexin VI-mediated loss of spectrin during coated pit budding is coupled to delivery of LDL to lysosomes. J. Cell Biol. **142:**937–947.
35. **Lin HC, Südhof TC, Anderson RG.** 1992. Annexin VI is required for budding of clathrin-coated pits. Cell **70:**283–291.
36. **Patterson S, Oxford JS, Dourmashkin RR.** 1979. Studies on the mechanism of influenza virus entry into cells. J. Gen. Virol. **43:**223–229.
37. **Matlin KS, Reggio H, Helenius A, Simons K.** 1981. Infectious entry pathway of influenza virus in a canine kidney cell line. J. Cell Biol. **91:**601–613.
38. **Monastyrskaya K, Babiychuk EB, Hostettler A, Wood P, Grewal T, Draeger A.** 2009. Plasma membrane-associated annexin A6 reduces Ca2+ entry by stabilizing the cortical actin cytoskeleton. J. Biol. Chem. **284:**17227–17242.
39. **Ohgami N, Ko DC, Thomas M, Scott MP, Chang CC, Chang TY.** 2004. Binding between the Niemann-Pick C1 protein and a photoactivatable cholesterol analog requires a functional sterol-sensing domain. Proc. Natl. Acad. Sci. U. S. A. **101:**12473–12478.
40. **Du X, Kumar J, Ferguson C, Schulz TA, Ong YS, Hong W, Prinz WA, Parton RG, Brown AJ, Yang H.** 2011. A role for oxysterol-binding protein-related protein 5 in endosomal cholesterol trafficking. J. Cell Biol. **192:**121–135.
41. **Millard EE, Gale SE, Dudley N, Zhang J, Schaffer JE, Ory DS.** 2005. The sterol-sensing domain of the Niemann-Pick C1 (NPC1) protein regulates trafficking of low density lipoprotein cholesterol. J. Biol. Chem. **280:**28581–28590.
42. **Barman S, Nayak DP.** 2007. Lipid raft disruption by cholesterol depletion

enhances influenza A virus budding from MDCK cells. J. Virol. **81:** 12169–12178.
43. **Rajendran L, Simons K.** 2005. Lipid rafts and membrane dynamics. J. Cell Sci. **118:**1099–1102.
44. **Suzuki T, Suzuki Y.** 2006. Virus infection and lipid rafts. Biol. Pharm. Bull. **29:**1538–1541.
45. **Gerke V, Moss SE.** 1997. Annexins and membrane dynamics. Biochim. Biophys. Acta **1357:**129–154.
46. **Backes P, Quinkert D, Reiss S, Binder M, Zayas M, Rescher U, Gerke V, Bartenschlager R, Lohmann V.** 2010. Role of annexin A2 in the production of infectious hepatitis C virus particles. J. Virol. **84:**5775–5789.
47. **Liscum L, Ruggiero RM, Faust JR.** 1989. The intracellular transport of low density lipoprotein-derived cholesterol is defective in Niemann-Pick type C fibroblasts. J. Cell Biol. **108:**1625–1636.
48. **Pagano RE.** 2003. Endocytic trafficking of glycosphingolipids in sphingolipid storage diseases. Philos. Trans. R. Soc. Lond. B Biol. Sci. **358:** 885–891.
49. **Mukherjee S, Maxfield FR.** 2004. Lipid and cholesterol trafficking in NPC. Biochim. Biophys. Acta **1685:**28–37.
50. **Lloyd-Evans E, Morgan AJ, He X, Smith DA, Elliot-Smith E, Sillence DJ, Churchill GC, Schuchman EH, Galione A, Platt FM.** 2008. Niemann-Pick disease type C1 is a sphingosine storage disease that causes deregulation of lysosomal calcium. Nat. Med. **14:**1247–1255.
51. **Veit M, Engel S, Thaa B, Scolari S, Herrmann A.** 2013. Lipid domain association of influenza virus proteins detected by dynamic fluorescence microscopy techniques. Cell. Microbiol. **15:**179–189.
52. **Rossman JS, Jing X, Leser GP, Lamb RA.** 2010. Influenza virus M2 protein mediates ESCRT-independent membrane scission. Cell **142:** 902–913.
53. **Domon MM, Matar G, Strzelecka-Kiliszek A, Bandorowicz-Pikula J, Pikula S, Besson F.** 2010. Interaction of annexin A6 with cholesterol rich membranes is pH-dependent and mediated by the sterol OH. J. Colloid Interface Sci. **346:**436–441.
54. **Ayala-Sanmartin J.** 2001. Cholesterol enhances phospholipid binding and aggregation of annexins by their core domain. Biochem. Biophys. Res. Commun. **283:**72–79.
55. **Müller KH, Kakkola L, Nagaraj AS, Cheltsov AV, Anastasina M, Kainov DE.** 2012. Emerging cellular targets for influenza antiviral agents. Trends Pharmacol. Sci. **33:**89–99.
56. **Walsh KB, Teijaro JR, Wilker PR, Jatzek A, Fremgen DM, Das SC, Watanabe T, Hatta M, Shinya K, Suresh M, Kawaoka Y, Rosen H, Oldstone MB.** 2011. Suppression of cytokine storm with a sphingosine analog provides protection against pathogenic influenza virus. Proc. Natl. Acad. Sci. U. S. A. **108:**12018–12023.
57. **Teijaro JR, Walsh KB, Cahalan S, Fremgen DM, Roberts E, Scott F, Martinborough E, Peach R, Oldstone MB, Rosen H.** 2011. Endothelial cells are central orchestrators of cytokine amplification during influenza virus infection. Cell **146:**980–991.
58. **Vandermeer ML, Thomas AR, Kamimoto L, Reingold A, Gershman K, Meek J, Farley MM, Ryan P, Lynfield R, Baumbach J, Schaffner W, Bennett N, Zansky S.** 2012. Association between use of statins and mortality among patients hospitalized with laboratory-confirmed influenza virus infections: a multistate study. J. Infect. Dis. **205:**13–19.
59. **Seyer R, Hrincius ER, Ritzel D, Abt M, Mellmann A, Marjuki H, Kühn J, Wolff T, Ludwig S, Ehrhardt C.** 2012. Synergistic adaptive mutations in the hemagglutinin and polymerase acidic protein lead to increased virulence of pandemic 2009 H1N1 influenza A virus in mice. J. Infect. Dis. **205:**262–271.